JOURNAL OF MATERIALS SCIENCE, 29 (1994) 6604 - 6610

Al_2O_3-5 wt % Al composites by ICP sintering of synthesized precursor

S. N. SINHA, S. H. KIM*
University of Illinois at Chicago, CEMM Department, M/C 246, PO Box 4348, Chicago, IL 60680, USA

Microstructure developments during the milling of Al_2O_3-5 wt % Al composite powder in an attritor and subsequent sintering of the precursor by inductively coupled argon plasma are presented. After 4 h of milling the precursor contained tubular ceramic–metal and uniform ceramic regions. With an increase in the milling period the ceramic–metal regions broke into smaller and almost globular regions, and the smaller regions became dispersed in the ceramic regions. After 8 h of milling the composite powder had a stable microstructure and contained 0.25–0.35 μm clusters. The sintered composite was > 99.7% dense and its microstructure consisted of ceramic–metal regions which were dispersed in the matrix of a ceramic region. The sizes of ceramic grains in ceramic–metal regions and the ceramic regions were 0.3–2.2 and 0.8–1.8 μm, respectively. Many ceramic grains in ceramic–metal regions were separated by 30–100 nm wide metal layers. The microstructure of the ceramic–metal region showed many features of interpenetrating phase composites. The Knoop and Vickers microhardnesses of the composites at 5–10 N loads were 410–450. Under 10 N loads in Knoop and Vickers' microhardness tests the crack length was 11 ± 3 and 3 ± 0.5 μm, respectively. The crack propogation mechanisms in the indented areas are discussed.

1. Introduction

In ceramic composites reinforcement of ceramic phases by metal or ceramic phases has been successfully used to increase their fracture toughness and impart R-curve behaviour [1–7]. In addition to reinforcement, interfaces play a dominant role in determining the mechanical properties of ceramic composites [6, 8–10]. Many processing approaches were deliberately designed to fabricate materials with customized interfaces [10–14].

Enhanced ductilities [15, 16] in nanocrystalline materials suggested that composites with nano-scale layers of constituent phases would exhibit resistance to plastic deformation well beyond the levels of monolithic homogeneous materials [15, 17]. Nano-scale layering of the constituent phases [18, 19] may account for the high ductility and strength in many naturally occurring biological composites. By layering of constituent phases the toughness and strength of many synthetic composites, e.g. B_4C–Al [13], Co–W [10, 11], Cu–Al [14], etc., were improved.

It appears that ceramic materials with optimally designed microstructures will have increased toughness values. The desired microstructures of such high performance materials will at least partly, if not completely, resemble those of interpenetrating phase composites (IPC). In IPCs each phase is continuous and interpenetrates throughout the microstructure [20]. The desired thickness of constituent phases in such high performance materials is less than 100 nm.

The IPC materials are new and the methods of producing such products are far from established [20]. The processing approaches that show varied potentials are based on: (1) spinodal decomposition; (2) use of materials with continuously interconnected porosity; (3) infiltration of a liquid phase into pre-existing open end preforms [20, 21]; (4) reduction of appropriate polycrystalline oxides from the metallic phases at grain boundaries [22]; (5) directed metal oxidation and related processes [23], etc.

During the fabrication of alumina based composites by using a recent two-stage processing approach [24], the precursor powder and sintered composite contained features typical of IPC materials. The first stage of the approach was an improved powder processing method in which a mixture of brittle (alumina) and ductile (aluminium) phases was milled in an attritior to synthesize a submicrometre precursor. In the second stage the precursor was cold-pressed without binder and the formed body was subsequently sintered by inductively coupled radio frequency plasma (ICP).

An earlier study demonstrated the feasibility of the approach for Al_2O_3–5 wt % Al composites. In the present approach the microstructure evolution of the composite powder in the milling stage are analysed. The characterization studies of the powders and the sintered compacts by scanning electron microscopy (SEM) and transmission electron microscopy (TEM) are included. During the micro-indentation test of the composites the interaction of crack with the

* Present addresss: Mechanical Engineering and Technology Department, Indiana Purdue University at Fort Wayne, IN 46805, USA.

0022–2461

microstructure are discussed. For the present experimental conditions the microstructure properties–interfacial characteristics–processing relationships are established.

2. Experimental procedure

Fig. 1 shows schematically the experimental route and the corresponding characterization studies. High purity (99.9% or better) α-alumina (1.5 μm) and aluminium powders (Johnson Mathey) were premixed in a roller–mixer for about 2 h. The premixed powder was milled in an attritor (Model 01-HD) union process. The milling media consisted of 5 mm diameter yttria-stabilized zirconia balls; a stainless steel tank and agitator were used. The ball:powder weight ratio was 10:1. During milling, the inside and outside of the milling tank were cooled by flowing argon gas and cold water, respectively. By cooling, the temperature rise of the powder during milling was limited to less than approximately 25 °C.

The powder was formed into 6.4 mm diameter cylinders by 280 MPa uniaxial pressure. No binder was added to the powder prior to forming. The formed sample was sintered by an ICP. The description of the ICP reactor is reported elsewhere [24].

The milled powder was characterized by SEM. The cluster sizes were estimated from the measurements of 20–30 clusters which were selected from ten or more SEM micrographs. The densities of the sintered samples were measured using Archimedes' principle. The sintered samples were characterized by optical microscopy, SEM and TEM. The Vickers and Knoop's microhardness numbers (H_V and H_K, respectively) were measured by Vickers' hardness tester, LECO, M400. Prior to microhardness tests, the samples were polished using 0.25 μm diamond grit. After the microindentation tests, the indented areas were examined by optical microscopy and SEM.

3. Results and discussion

In a series of milling experiments a mixture of Al_2O_3–5 wt % Al was milled for 2, 4, 8, 16 or 24 h. The milling conditions of the selected experiments are included in Fig. 1 and Table I.

3.1. Milled powder

The SEM micrographs of the powder showed that the powders consisted of clusters. Fig. 2 shows the typical nature of the clusters in a powder which was milled for 8 h. After 4 h of milling the range of cluster sizes was quite large: 0.25– > 1 μm. After 8 and 16 h of milling the cluster sizes were almost the same, 0.25–0.35 μm.

The XRD patterns of the powdered sample (not shown here) showed that, even after 16 h of milling, the chemical composition of the precursor did not change, but the XRD peaks of Al_2O_3 and Al phases broadened considerably. The broadening of peaks was

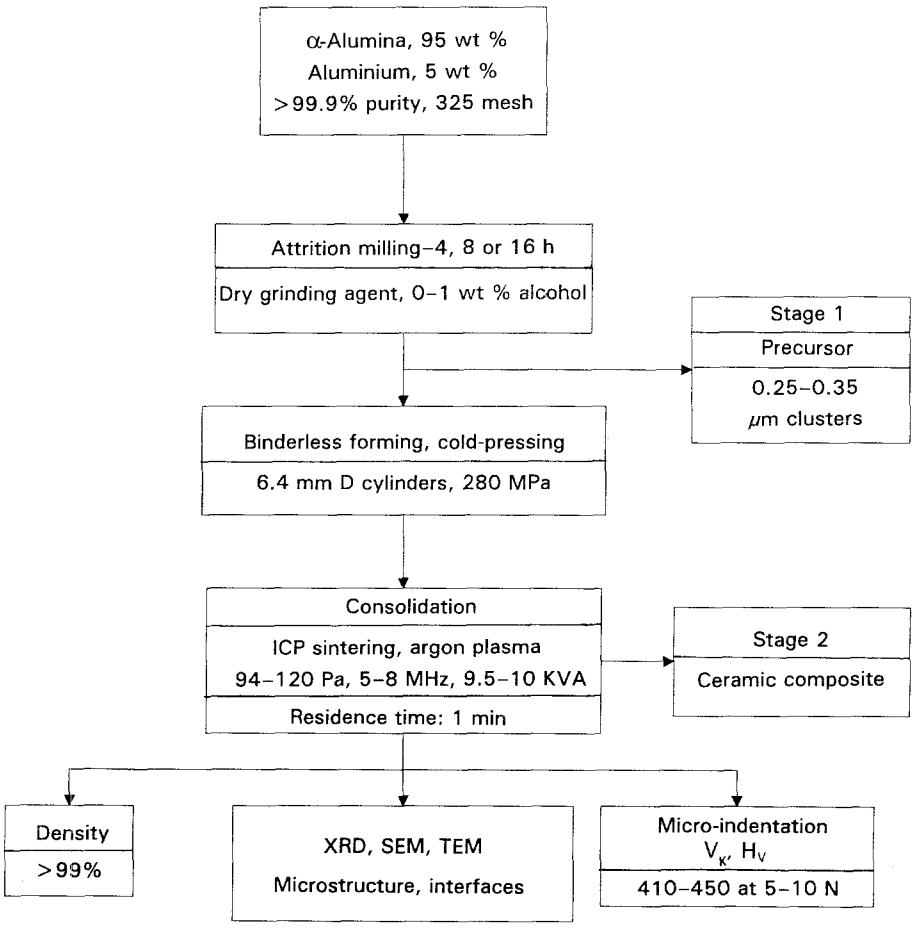

Figure 1 A schematic description of the processing conditions and characterization studies.

TABLE I The density and grain sizes of the ICP sintered Al_2O_3–5 wt % composites

Sample no.	Milling time (h)	Sintered sample				
		Density[a]		Ceramic (Al_2O_3) grain sizes (μm)		
		g cm^{-3}	Theoretical (%)	Ceramic region		Ceramic–metal region
				Average	Range	
CMC1	4	3.71	97.4	1.4	0.8–1.9	–
CMC2	8	3.80	99.7	1.2	0.8–1.5	0.3–2.2
CMC3	16	3.81	100.0	1.2	0.8–1.4	0.3–2.0

[a] Theoretical density was 3.81 g cm^{-3}, which was calculated by using the rule of the mixtures and the composition of the starting materials. The average density values of five measurements are included. In CMC2 and CMC3 the density values ranged from 3.78 to 3.84 and 3.76 to 3.84 g cm^{-3}, respectively.

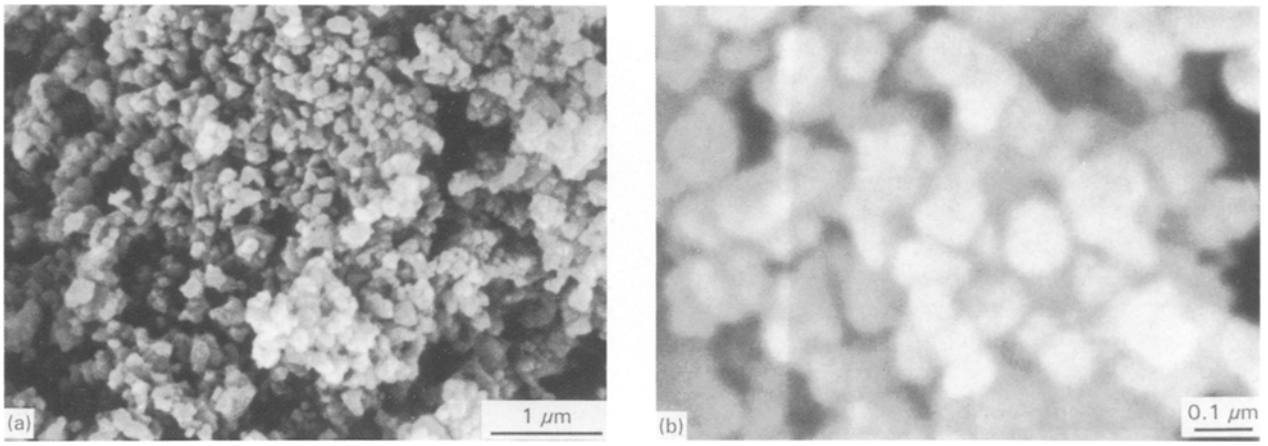

Figure 2 SEM micrographs of the precursor in CMC2. The precursor was milled for 8 h. The markers are in micrometres. The clusters of particles are visible.

due to residual strains in the lattice caused by milling and the submicrometre sizes of the particles. From the broadened peaks the calculated sizes of the alumina particles were 30–100 nm (± 30%) [25].

3.2. Microstructures of ICP sintered composites

Optical micrographs of the sintered samples (CMC1, CMC2 and CMC3) are shown in Fig. 3a–c. In CMC1, CMC2 and CMC3, the precursor was milled for 4, 8 and 16 h, respectively, and the sintering conditions were identical (see Fig. 1 and Table I).

The microstructures showed two broad regions, dark and bright areas. The detailed microstructures of these regions revealed (discussed later) that the dark and bright regions corresponded to the ceramic matrix (which contained a uniform dispersion of ceramic grains) and a ceramic–metal region (which comprised of ceramic grains and a small amount of metal phase), respectively. With increased milling times, the general characteristics of dark areas (matrix) did not change but those of bright areas changed considerably.

In Fig. 3a, where the precursor was milled for 4 h, the following three geometric configurations of bright areas are visible: (1) 20–50 μm long, 3–10 μm wide (possibly tubular) areas; (2) 3–10 μm long, 3–5 μm wide (possibly tubular) areas; and (3) 2–3 μm wide, relatively globular areas. The relative dispersion of the areas with a geometric configuration [(3)] in the matrix was much more uniform than those with configurations (1) or (2).

In Fig. 3b, where the precursor was milled for 8 h, the bright areas with long tubular configuration [(1) and (2) in Fig. 3a] were absent and the maximum widths of globular bright areas [(3)] in Fig. 3a had shrunk to about 1 μm. Also, the globular bright areas were more evenly dispersed than in Fig. 3a in the matrix.

In CMC3 (Fig. 3c), in which the precursor was milled for 16 h, the globular bright areas became slightly smaller and more evenly dispersed in the matrix than those in CMC2.

For the present experimental conditions, 8 h of milling was adequate to obtain a fairly uniform dispersion of ceramic–metal regions in the matrix of uniform ceramic regions.

3.3. Ceramic–metal and uniform ceramic regions of the composite

The salient features of ceramic–metal and ceramic regions are highlighted in the SEM micrographs of CMC2 samples (Fig. 4a–c). A typical SEM micrograph (Fig. 4a) of the composite at low magnification

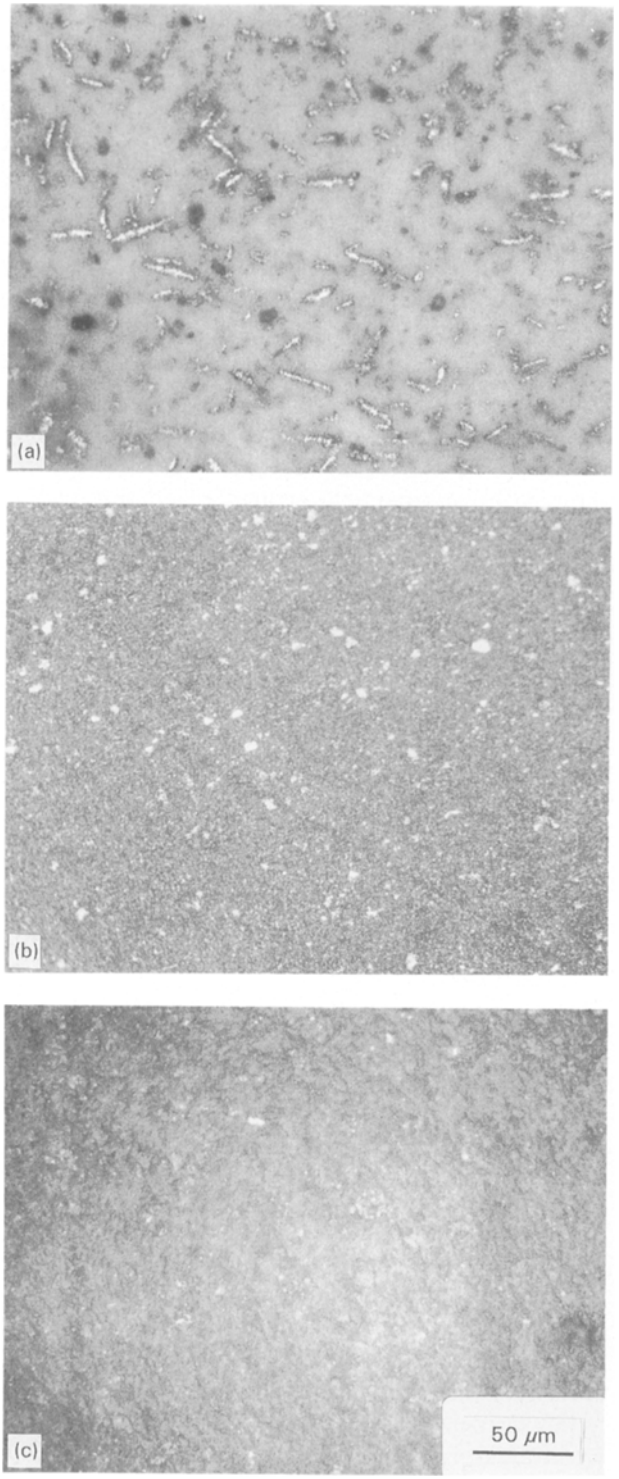

Figure 3 Optical micrographs of ICP sintered samples. Prior to sintering, the precursor was milled for 4 h (a), 8 h (b) and 16 h (c). The sintering conditions were same in all cases. The figures show the approximate shapes of ceramic–metal (bright) and uniform ceramic (dark/background) regions.

(< 5000) showed that the ceramic–metal regions had globular shapes and were well dispersed in the ceramic matrix. In Fig. 4a the sample was roughly polished to preserve the ceramic–metal regions. In Fig. 4b and c the samples were fine polished with diamond paste. Fig. 4b and c highlight the microstructures of the uniform regions and the ceramic–metal regions, respectively. In ceramic–metal areas well-sintered ceramic grains were almost "glued" by small amounts of metal phases. In uniform regions the well-sintered ceramic grains were touching each other. No metal phase was detected in the uniform regions.

Fig. 5a and b show the TEM micrographs of uniform and ceramic–metal regions respectively in CMC2. TEM micrographs showed that the ceramic grains in ceramic–metal as well as uniform ceramic regions were well sintered. Furthermore, many ceramic grains in ceramic–metal regions were separated by thin metal layers.

The ceramic–metal regions of Al_2O_3–5 wt % composites in Figs 4 and 5 exhibited the following characteristics of IPC microstructures: in IPC materials each

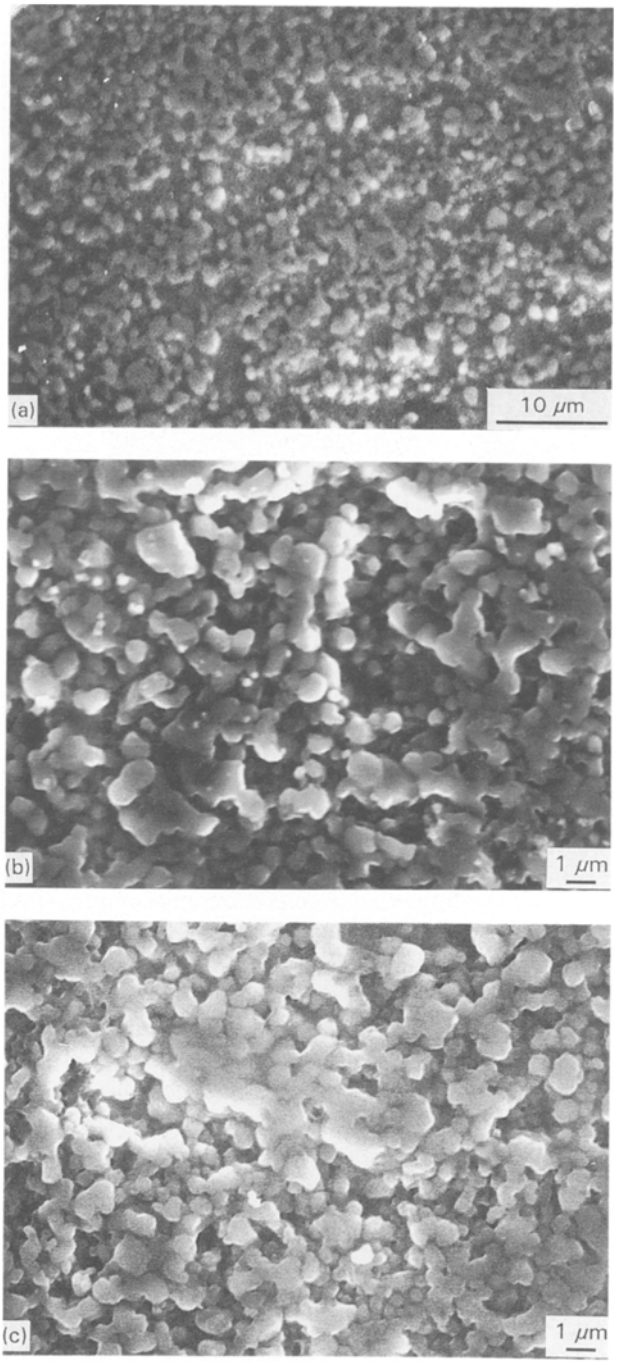

Figure 4 SEM micrographs of the composite CMC2 in which the precursor was milled for 8 h. (a) The ceramic–metal regions appear as rounded areas, the background is the ceramic region. (b) and (c) highlight the ceramic–metal and uniform ceramic regions, respectively.

Figure 5 TEM micrographs of CMC2 composites from (a) ceramic–metal and (b) ceramic regions. In both regions the ceramic grains were well sintered. The bright area in (a) indicates the metal phase.

phase was continuous and interpenetrated throughout the microstructures. In the present case the ceramic–metal regions were not continuous throughout the matrix, but were uniformly dispersed in the ceramic matrix. In limited areas of ceramic–metal regions a continuous network of metal phase formed around ceramic grains. The microstructures in Figs 3–5 had the following architecture: micrometre-sized regions with limited IPC type microstructures uniformly dispersed in a matrix of a well-sintered ceramic phase.

One unusual feature of the ceramic–metal interfaces in Fig. 5b is that the metal layers between ceramic grains were relatively uniform and continuous. The alumina phase was not wetted by the liquid aluminium phase. Hence, the geometric configurations were not expected in the equilibrium condition. Such interfacial characteristics are essential to form IPC microstructures. Thus, the present method would have inherent advantages in fabricating ceramic IPC materials.

3.4 Milling time–microstructure relationships of the precursor

Corresponding to ceramic–metal and uniform ceramic regions in the sintered products, there were comparable ceramic–metal and uniform ceramic regions in the powdered precursor. It was reasonable to assume that same sintering conditions during ICP sintering of CMC1, CMC2 and CMC3 would cause similar changes in the geometric configurations of ceramic–metal and ceramic regions of the powder.

From the microstructure milling time relationships of ceramic–metal and uniform ceramic regions of CMC1–CMC3 the following relationship between the microstructural architecture of the precursor and milling time is estimated. During early stages of milling (< 4 h in the present case) there were two distinct regions in the precursor: (1) ceramic–metal regions where ceramic particles were "glued" together with the metal phases and (2) clusters of ceramic particles. The optical micrograph of CMC1 (Fig. 3a) showed the approximate geometry and the relative dispersion of these two regions. As the milling time increased the geometric configuration of the ceramic–metal regions changed from tubular to more rounded and smaller shapes. Also, the number of ceramic–metal regions per unit volume increased. It appeared that as the milling continued to increase then the tubular regions in the early stages broke into smaller regions and the smaller ceramic–metal regions became progressively dispersed in the matrix of uniform ceramic regions. The sizes of the ceramic–metal regions in the powder were unknown.

3.5. Density and grain size of the sintered compact

The density of the sintered compacts are listed in Table I. The theoretical density of the sintered compact was 3.81 $g\,cm^{-3}$ – calculated using the rule of mixtures and density values of pure alumina and aluminium phases of 3.89 and 2.70 $g\,cm^{-3}$, respectively [26]. It was further assumed that the amount of metal phase in the composite was the same as in the starting materials of the milling stage. The latter assumption may be in error because the metal content may have increased due to reducing conditions in ICP sintering [27], decreased due to volatilization during the ICP sintering stage or changed due to unknown reasons. However, since the metal content of the starting materials was only 5 wt %, the absolute value of the error would be insignificant.

Table I indicates that CMC2 and CMC3 were sintered to about 99.7 and 100% of their theoretical densities, respectively. Even at a magnification of 100 000, SEM micrographs of the composites did not show any void or porosity.

The grain size was calculated by statistical methods. In each of ten or more different regions the sizes of 20–30 grains were measured from SEM micrographs. The grain sizes of the alumina grains in the uniform and ceramic–metal regions are included in Table I. In the few TEM micrographs that were observed, the maximum thickness of metal layers between two adjacent ceramic grains (in ceramic–metal regions) ranged from 30 to 100 nm, approximately.

ICP sintering of alumina has already been reported [28–30]. Starting from 0.3 μm particles, alumina powder and an Al_2O_3–0.25% MgO mixture have been

sintered by ICP to 96 and 99.7% of their theoretical densities, respectively [28]. A similar powder was sintered by microwave plasma to 99.8% density with a grain size of 2 μm [28]. For MgO-doped alumina with 99.7% density the grain size was about 3 μm. A recent paper [30] reported the grain sizes of ICP sintered high purity alumina to be 0.2–0.7 μm. To the best of the authors' knowledge, except in their preliminary work [24], the ICP sintering of Al_2O_3–5 wt % Al or comparable composites has not been reported.

Although the grain sizes of ceramic grains were quite small in ICP sintered Al_2O_3–5 wt % Al composites, the ratio of ceramic grain sizes: ceramic particle sizes in the precursor was much larger than those in earlier studies of ICP sintering of alumina [28, 30]. It appeared that by optimizing the processing parameters further decreases in the grain sizes were possible.

3.6. Microhardness tests

The microhardnesses of the sintered samples in ambient conditions are shown in Fig. 6. At 0.5 (5 N) and 1.0 (10 N) kg indentation weights H_V and H_K values were 410–450. The hardness of the ICP sintered composites were comparable to those of Al_2O_3–20 vol % Al Lanxide™ composites [31].

After the microhardness tests the indented areas were examined by SEM, enabling the crack lengths to be measured. At 500 g indentation weights the SEM micrographs (10 000 magnification) of the indented areas showed no cracks. SEM micrographs of the indented areas at 1 kg (10 N) micro-indentation weight are shown in Fig. 7. At 1 kg of load the lengths of cracks in the Vickers and Knoop tests were 11 ± 3 and 3 ± 0.5 μm, respectively.

In both tests the following crack propagation mechanisms were observed: (1) intergranular, in alumina grains; (2) interfacial, through alumina/aluminium metal interfaces; (3) transgranular through alumina and aluminium phases. Also, considerable bridging of cracks was visible. It appeared that propagation of cracks occurred through almost every possible mechanisms [7]. The probable cause was the microstructural architecture of the sintered compact: the composite comprised of ceramic–metal regions with limited IPC microstructure and the ceramic–metal regions were dispersed in a uniform ceramic matrix. The geometric constraints of such an architecture would force the crack to propagate through and across ceramic or metal grains and interfaces.

The crack lengths obtained in micro-indentation tests were quite small. Hence, the composites would have high fracture toughness values. In the absence of measured Young's modulus values, the fracture toughness from the observed crack lengths in the micro-indentation tests were not estimated.

4. Summary and conclusions

1. By milling a mixture of Al_2O_3–5 w % Al in an attritor a composite powder was synthesized. During early stages of milling (4 h or less) the precursor consisted of tubular shapes of ceramic–metal regions and uniform ceramic regions. As the milling was continued the ceramic–metal regions from the early stages broke into smaller regions and the smaller regions become progressively dispersed in the ceramic matrix. Beyond 8 h of milling the microstructure of the precursor did not change significantly. The cluster sizes in the precursor with the stable microstructure ranged from 0.25 to 0.35 μm. For the present experimental condition the optimum milling period was 8 h.

2. In the microstructures of the ICP-sintered composites, ceramic–metal regions were dispersed in the matrix of a uniform ceramic phase. The sintered composite CMC1, in which the precursor was milled for 4 h, exhibited two distinct geometric configurations of ceramic–metal regions: 20–50 μm long and 3–10 μm wide tubular areas, and 3–10 μm long and 3–5 μm wide tubular areas. The ceramic–metal regions of

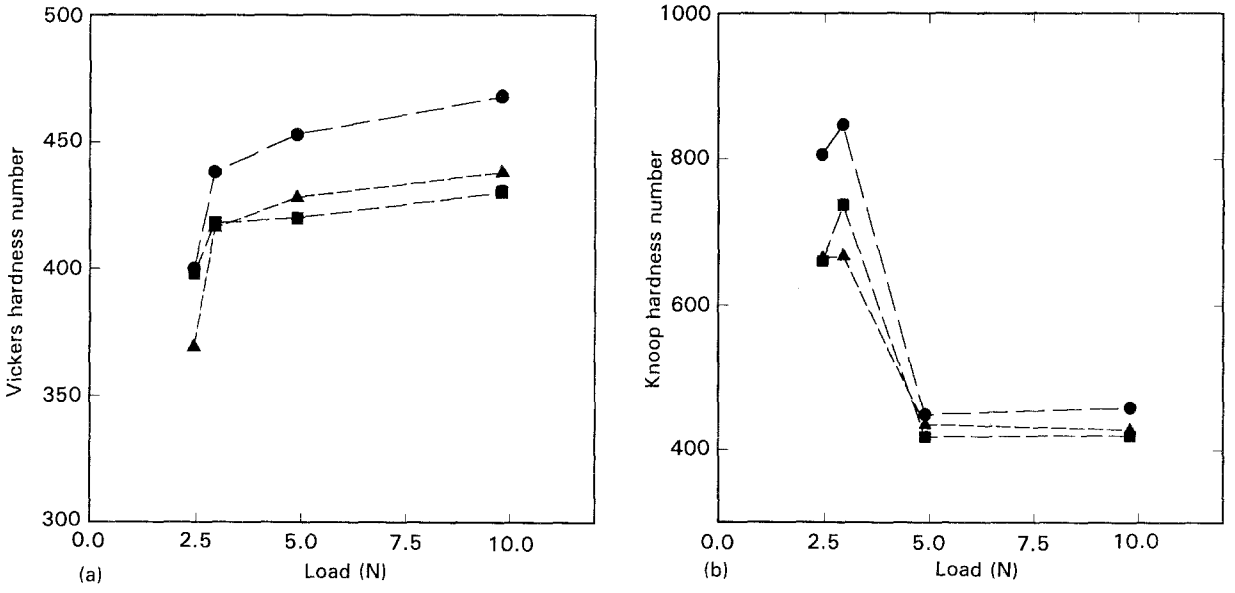

Figure 6 The Vickers (a) and Knoops (b) microhardness of the sintered samples. ●, CMC1; ▽, CMC2; ▼, CMC3.

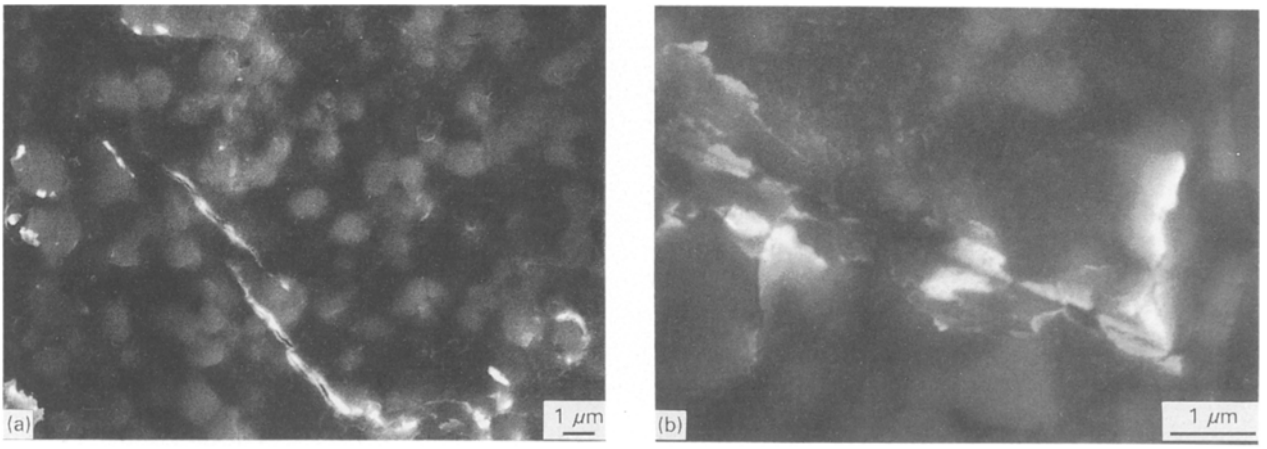

Figure 7 SEM micrographs of the indented areas from the H_V (a) and H_K (b) tests at 1 kg indentation loads. The samples were from CMC2. The cracks were propagated through almost every possible route: transgranular and intergranular in ceramic and metal phases, as well as along ceramic metal–interfaces.

CMC2 and CMC3, in which the milling period of the corresponding precursor was 8 and 16 h, respectively, were almost globular, smaller (about 1 μm) and uniformly dispersed in the ceramic matrix.

3. In ceramic–metal regions of CMC2, the grain sizes of the ceramic grains were about 0.3–2.2 μm and many ceramic grains were separated by 30–100 nm wide metal layers. The microstructural architecture of the ceramic–metal regions showed many features of IPC materials. In ceramic regions no metal phase was detected and the grain sizes ranged from 0.8 to 1.8 μm.

The microstructures of Al_2O_3–5 wt % Al composites had the following approximate architecture: micrometre sized ceramic–metal regions with limited IPC microstructures uniformly dispersed in a ceramic phase.

4. The composites CMC2 and CMC3 were more than 99.7% dense. At 1.0 and 0.5 kg indentation loads, the H_V and H_K micro-hardnesses of CMC2 and CMC3 were 410–450.

5. After micro-indentation tests at 1 kg load, the crack lengths in Knoop and Vickers' micro-hardness tests were only 11 ± 3 and 3 ± 0.5 μm, respectively. In the indented areas intergranular and transgranular cracks through ceramic and metal phases were observed. Many cracks propagated through metal–ceramic interfaces. Also, considerable bridging of cracks was visible.

References

1. L. S. SIGL and H. E. EXNER, *Acta Metall.* **37** (1989) 1847.
2. F. F. LANGE, B. V. VELAMAKANNI and A. G. EVANS, *J. Amer. Ceram. Soc.* **73** (1990) 383.
3. N. CLAUSSEN, N. A. TRAVITZKY and S. WU, *Ceram. Engng. Sci. Proc.* **11** (1990) 806.
4. M. MANOHARAN, L. ELLIS and J. J. LEWANDOWSKI, *Scripta Metall.* **24** (1990) 1515.
5. A. J. PYZIK, A. A. AKSAY, M. SARIKAYA, in Proceedings of Ceramic Microstructures '86, Roles of Interfaces, edited by J. A. Pask and A. G. Evans (Plenum Press, NY, 1987) p. 45.
6. H. J. EDREES and A. HENDRY, in "Interfacial behavior in ceramic matrix composites with metal particles" (Butterworth, London, 1989) p. 297.
7. A. G. EVANS, *J. Amer. Ceram. Soc.* **73** (1990) 187.
8. J. A. CORNIE, *MRS Bull.* **16** (1991) 27.
9. D. A. WEIRAUCH JR, *J. Mater. Res.* **3** (1988) 729.
10. C. G. LEVI, G. J. ABBASCHIAN and R. MEHRABLAN, *Met. Trans.* **9A** (1989) 697.
11. E. BREVAL, M. K. AGHAJANIAN and S. L. LUSZCZ, *J. Amer. Ceram. Soc.* **73** (119) 2610.
12. P. G. KARANDIKAR and T. CHOU, *J. Mater. Sci.* **26** (1991) 2573.
13. A. G. GENSING, G. BURGER, E. LUCE, N. CLAUSSEN, S. WU and N. A. TRAVITZKY, *Ceram. Engng. Sci. Proc.* **11** (110) 806.
14. S. WU and N. CLAUSSEN, *J. Amer. Ceram. Soc.* **74** (1991) 2460.
15. F. H. FROES and C. SURYANARAYANA, *JOM* **6** (1989) 12.
16. B. H. KEAR, L. E. CROSS, J. E. KEEM, R. W. SIEGEL, F. SPAEPEN, K. C. TAYLOR, E. L. THOMAS and K. N. TU, "Research opportunities for materials with submicron sized microstructures" (NMAB-454, National Academy Press, 1989).
17. S. L. LEHOCZKY, *J. Appl. Phys.* **49** (1978) 5479.
18. I. A. AKSAY and M. SARIKAYA, "Processing of synthetic hierarchically structured ceramic-based materials", Presented at the Symposium of "Hierarchically structured materials", MRS, Fall 1991 Meeting, Boston, Dec. 2–5 (1991).
19. S. L. LEHOCZKY, *Phys. Rev. Lett.* **41** (1978) 1814.
20. D. R. CLARKE, *J. Amer. Ceram. Soc.* **75** (1992) 735.
21. D. C. HENDERSON, A. J. PYZIK, I. A. AKSAY and W. E. SNOWDEN, *J. Amer. Ceram. Soc.* **72** (1989) 775.
22. M. I. MENDELSON and M. E. FINE, *J. Amer. Ceram. Soc.* **57** (1974) 154.
23. M. S. NEWKIRK, H. D. LESHER, D. R. WHITE, C. R. KENNEDY, A. W. URQUART and T. D. CLAAR, *Ceram. Engng. Sci. Proc.* **8** (1987) 879.
24. S. H. KIM and S. N. SINHA, *Ceram. Engng. Sci. Proc.* **13** (1992) 855.
25. E. SWEET and S. N. SINHA, Unpublished work.
26. *Ceramic Source* (American Ceramic Society) **8** (1992) TD37.
27. C. A. KOTECKI, M.S. Thesis, Northwestern University (1987).
28. J. S. KIM and D. L. JOHNSON, *Amer. Ceram. Bull.* **62** (1983) 620.
29. K. UPADHYA, *Ceram. Bull.* **67** (1988) 1691.
30. J. D. HANSEN, R. RUSTIN, M. H. TENG and D. L. JOHNSON, *J. Amer. Ceram. Soc.* **75** (1992) 1129.
31. S. M. BHADURI and F. H. FROES, *JOM* **43** (1991) 16.

Received 15 December 1992
and accepted 21 March 1994